PHYSICAL REVIEW B **78**, 174526 (2008)

Crossover from *hc*/*e* to *hc*/2*e* current oscillations in rings of *s*-wave superconductors

F. Loder, A. P. Kampf, and T. Kopp
Center for Electronic Correlations and Magnetism, Institute of Physics, University of Augsburg, D-86135 Augsburg, Germany
(Received 22 August 2008; published 25 November 2008)

We analyze the crossover from an *hc*/*e* periodicity of the persistent current in flux-threaded clean metallic rings toward an *hc*/2*e*-flux periodicity of the supercurrent upon entering the superconducting state. On the basis of a model calculation for a one-dimensional ring we identify the underlying mechanism, which balances the *hc*/*e* versus the *hc*/2*e* periodic components of the current density. When the ring circumference exceeds the coherence length of the superconductor, the flux dependence is strictly *hc*/2*e* periodic. Further, we develop a multichannel model which reduces the Bogoliubov–de Gennes equations to a one-dimensional differential equation for the radial component of the wave function. The discretization of this differential equation introduces transverse channels whose number scales with the thickness of the ring. The periodicity crossover is analyzed close the critical temperature.

DOI: 10.1103/PhysRevB.78.174526 PACS number(s): 74.20.Fg, 74.25.Fy, 74.25.Sv, 74.62.Yb

I. INTRODUCTION

Charged particles, which encircle a magnetic flux-threaded region, acquire a geometric phase. This Aharonov-Bohm (AB) phase leads to quantum interference phenomena along multiply connected paths.[1] A particular manifestation of the AB effect is the persistent current in mesoscopic metal rings,[2,3] which is modulated periodically by the magnetic flux piercing the interior of the ring with the period of a flux quantum $\Phi_0 = hc/e$ for clean rings.

Likewise, in superconducting rings the order parameter responds periodically to magnetic flux as implied by the requirement of a single-valued superconducting wave function in the presence of a supercurrent.[4–6] Measurements of magnetic flux trapped in small cylinders proved that the flux in superconductors is quantized in units of $\Phi_0/2$.[7,8] The *hc*/2*e* superconducting flux quantum was corroborated by measurements of the *hc*/2*e* periodicity of the critical temperature of superconducting rings by Little and Parks[9,10] and by the *hc*/2*e* flux quantization of Abrikosov vortices.[11]

The oscillations of the persistent current or the supercurrent with respect to the magnetic flux imply the corresponding periodicity for all thermodynamic functions.[12] Two classes of condensate states have been identified which are not related by a gauge transformation. In the thermodynamic limit, they are degenerate for integer and half-integer flux values, which results in the observed $\Phi_0/2$ periodicity. This degeneracy is however lifted for discrete systems,[13] which was implicitly understood already in the early works of Byers and Yang[5] and by Brenig.[14] The lifting of the degeneracy can be made explicit through the evaluation of the supercurrent in sufficiently small rings.[15] Recently, nodal superconductors have been in the focus of research[15–18] as they allow for striking differences in the excitation spectrum for flux sectors centered around integer and half-integer Φ_0 values, respectively.

For rings of *s*-wave superconductors, it is expected that the *hc*/*e* periodicity is restored if the ring diameter is smaller than the coherence length.[15,19–21] While the Φ_0 and the $\Phi_0/2$ periods are well understood in metallic and superconducting rings, it has remained unaddressed how the periodicity evolves for such a small ring when the normal metal turns superconducting. Here we analyze the periodicity crossover in a one-dimensional (1D) model for a flux-threaded ring at zero temperature, which allows for a transparent analytical treatment on the basis of the Gor'kov equations in an external magnetic field (Sec. II).

The gap equation for the current carrying superconducting state is solved for finite-size rings to evaluate the field dependence of the discrete energy spectrum and the supercurrent. We identify two components of the current with *hc*/*e* and *hc*/2*e* periodicities, respectively, whose magnitudes shift with the opening and increase in the energy gap in the superconducting state. When the coherence length of the superconducting ring is of the order of the ring size, only the *hc*/2*e*-periodic component remains. A similar analysis for the temperature-driven crossover in clean and dirty 1D rings was recently published by Wei and Goldbart.[20]

It is well known that a long-range-ordered superconducting state does not exist in 1D. However, whereas thermal phase slips suppress a transition into the superconducting state at finite temperature, quantum phase slips at zero temperature are rare events. Even if phase coherence is broken at certain instants in time and space, the supercurrent does not decay in the ring. We therefore investigate only the zero-temperature transition for the 1D ring.

Subsequently (Sec. III) we extend our analysis to rings of finite thickness ("annuli"), which represent, from a formal point of view, multichannel systems. For the annuli we present the periodicity crossover upon cooling through the superconducting transition temperature. For annular systems that are confined to a two-dimensional (2D) plane, we introduce a semianalytical approach in which the numerical work is reduced to the solution of a one-dimensional differential equation for the radial component of the wave function. Its discretization allows us to introduce a fixed number of (transverse) channels whose number parametrizes the thickness of the annulus.

II. 1D RING

We start from the tight-binding form of the kinetic energy for a 1D ring with N sites as given by

$$\mathcal{H}_0 = -t \sum_{\langle ij\rangle,s} e^{\varphi_{ij}} c_{js}^\dagger c_{is}, \tag{1}$$

where the sum extends over all nearest-neighbor sites i and j, $s=\uparrow,\downarrow$ denotes the spin, and t is the hopping matrix element. The vector potential $\mathbf{A}$ of an external magnetic field enters through the Peierls phase factor, $\varphi_{ij}=(e/\hbar c)\int_i^j \mathbf{A}\cdot d\mathbf{r} = 2\pi\phi/N$, where $\phi=\Phi/\Phi_0$ and Φ is the magnetic flux through the ring. After Fourier transformation $\mathcal{H}_0$ becomes

$$\mathcal{H}_0 = \sum_{ks} \epsilon_{k-\phi} c_{ks}^\dagger c_{ks}, \tag{2}$$

with the single-particle energy for a state with angular momentum $\hbar k$,

$$\epsilon_{k-\phi} = -2t \cos\left(\frac{k-\phi}{R}\right). \tag{3}$$

$R=N/2\pi$ denotes the dimensionless radius of the ring and $k=-N/2,\ldots,N/2-1$. If N is a multiple of 4, a k value exists for which $\epsilon_k=0$,[22] with two states exactly at the Fermi energy $E_F=0$ for $\phi=0$. To ensure a unique ground state, we choose $\mu=t/N$ which is placed in between two single-particle energies ϵ_k. This is achieved for even N, which are not multiples of 4. All calculations were performed for this generic choice of N and μ.

The superconducting state in this strictly 1D ring model is controlled by a BCS-type Hamiltonian of the form

$$\mathcal{H} = \mathcal{H}_0 + \sum_{k,q} [\Delta_k^*(q) c_{-k+q\downarrow} c_{k\uparrow} + \Delta_k(q) c_{k\uparrow}^\dagger c_{-k+q\downarrow}^\dagger], \tag{4}$$

where $\Delta_k(q)$ is the superconducting order parameter for the formation of Cooper pairs with finite angular momentum $\hbar q$ and $q\in\mathbb{Z}$. The order parameter is obtained from the anomalous imaginary time Green's function $F(k,k',\tau-\tau') = \langle T_\tau c_{k\downarrow}(\tau) c_{-k'\uparrow}(\tau')\rangle$ (Ref. 23) by

$$\Delta_k(q) = k_B T \sum_{k'} \sum_n V_{kk'} F(k', k'-q, \omega_n), \tag{5}$$

where $\omega_n=(2n-1)\pi k_B T$ is the fermionic Matsubara frequency for temperature T, $V_{kk'}$ is the pairing interaction, and T_τ is the time-ordering operator.

$\Delta_k(q)$ has to be determined self-consistently in the superconducting state. This is achieved by solving the equations of motion for the anomalous Green's function and the single-particle propagator $G(k,\tau-\tau')=\langle T_\tau c_{ks}(\tau) c_{ks}^\dagger(\tau')\rangle$, which is diagonal with respect to momentum and spin. This leads to the self-consistent set of Gor'kov equations,

$$G^{-1}(k,\omega_n) = G_0^{-1}(k,\omega_n) + \sum_q \Delta_k(q) G_0(-k+q,-\omega_n) \Delta_{k-q}^*(q), \tag{6}$$

$$F(k,k-q,\omega_n) = G_0(k,\omega_n)\Delta_k(q) G(-k+q,-\omega_n), \tag{7}$$

where $G_0(k,\omega_n)=[i\hbar\omega_n-\epsilon_{k-\phi}]^{-1}$ is the Green's function in the normal state.

We assume that the unique ground state of the superconducting condensate is characterized by a single integer quantum number $q(\phi)$. For rings larger than the coherence length, the q number of the ground state advances to the next integer whenever ϕ crosses the flux values $(2n-1)/4$, with $n\in\mathbb{Z}$, i.e., $q(\phi)=\text{floor}(2\phi+1/2)$, where floor$(x)$ is the largest integer smaller than x. Discreteness of the energy levels shifts the increment in q slightly according to the energy difference of even-q and odd-q states. Disregarding this small shift in the first approach (see comment at the end of this section), we take $\Delta_k(q)$ of the form

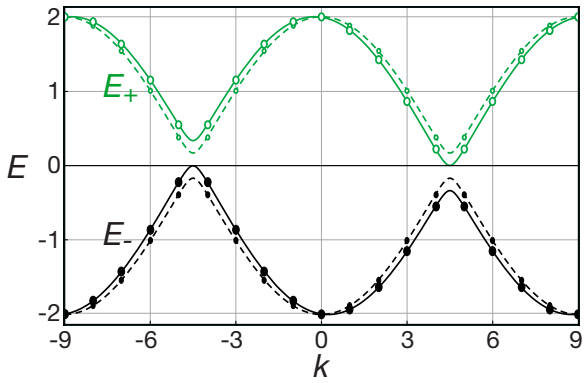

FIG. 1. (Color online) Energy dispersion of a ring with an order parameter $\Delta=0.22t$ for $\phi=0$ (dashed line) and $\phi=\phi_c\approx 0.24t$ (solid line), where the indirect energy gap closes. The filled (empty) circles represent occupied (unoccupied) k states for a ring with $N=18$. The asymmetry for $\pm k$ scales with $1/R$.

$$\Delta_k(x) = \delta(x-q(\phi))\Delta_k. \tag{8}$$

For s-wave pairing, which is the only Cooper-pair state possible in a strictly 1D system, $\Delta_k\equiv\Delta$ is constant. With this ansatz, we determine the Green's function from Eq. (6) as

$$G(k,\omega_n) = \frac{-i\hbar\omega_n - \epsilon_{-k-\phi+q}}{[i\hbar\omega_n - E_+(k,\phi)][i\hbar\omega_n - E_-(k,\phi)]}, \tag{9}$$

where the two energy branches $E_\pm(k,q)$ are given by

$$E_\pm(k,\phi) = \frac{\epsilon_{k-\phi}-\epsilon_{-k-\phi+q}}{2} \pm \sqrt{\Delta^2+\epsilon^2(k,\phi)}, \tag{10}$$

with $\epsilon(k,\phi)=(\epsilon_{k-\phi}+\epsilon_{-k+q-\phi})/2$. The energies $E_\pm(k,\phi)$ are plotted in Fig. 1 as a function of k. The upper (E_+) and the lower branches (E_-) are separated by an indirect energy gap, which closes at a critical value Δ_c. For finite flux the dispersion is asymmetric with respect to an inversion in the angular momentum $k\to -k$ (see Fig. 1), and this asymmetry induces a finite supercurrent. In the "small-gap" regime $\Delta<\Delta_c$, both $E_+(k,\phi)$ and $E_-(k,\phi)$ can be positive or negative, whereas in the "large-gap" regime $\Delta>\Delta_c$, $E_+(k,\phi)>0$ and $E_-(k,\phi)<0$ for all k and ϕ [see Fig. 2(a)]. Close to E_F, $E_\pm(k,\phi)$ simplifies to

$$E_\pm(\pm k,\phi) \approx \mp \frac{t}{R}(2\phi-q) \pm \sqrt{\Delta^2+l(t/R)^2}, \tag{11}$$

where $k>0$, $l=1$ for even q, and $l=0$ for odd q. The maximum direct energy gap in the even-q sectors is therefore $\Delta_0=\sqrt{\Delta^2+(t/R)^2}$, whereas in the odd-$q$ sectors it is $\Delta_{1/2}=\Delta$. Equation (11) shows that the shift of the eigenenergies scales with the ring size as $1/R$ in the small-gap regime.

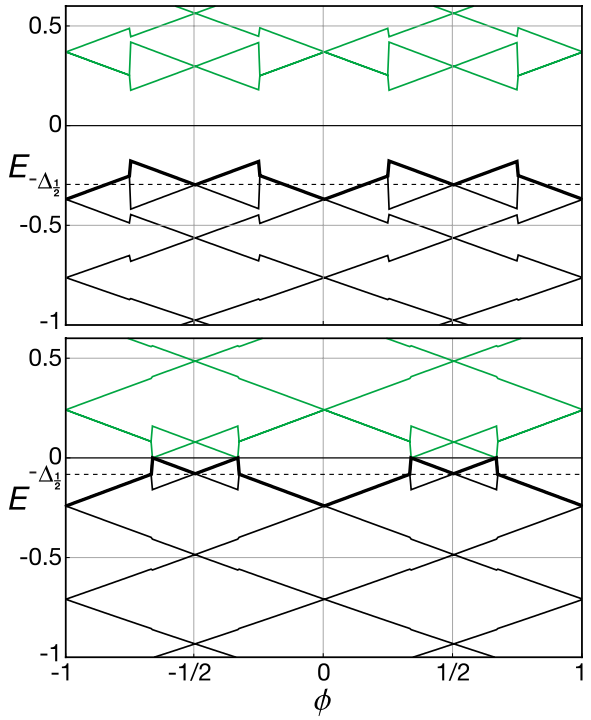

FIG. 2. (Color online) Eigenenergies $E_{\pm}(k,\phi)$ [Eq. (10)] as a function of flux ϕ for $N=26$ and a self-consistently calculated order parameter Δ; lines below $E=0$: $E_{-}(k,\phi)$ and lines above $E=0$: $E_{+}(k,\phi)$. Upper panel: large-gap regime ($V=1.9t$ and $\Delta_{1/2}\approx 0.30t$). Lower panel: small-gap regime ($V=1.1t$ and $\Delta_{1/2}\approx 0.08t$). Superconductivity occurs only in the odd-q sectors for $V=1.1t$ (see Fig. 3). The bold line marks the highest occupied state for all ϕ. For the definition of $\Delta_{1/2}$ see text after Eq. (11).

By inserting $G(k,\omega_n)$ into the Gor'kov equation (7), one finds for the anomalous Green's function,

$$F(k,k-q,\omega_n)=\frac{\Delta(\phi)}{[i\hbar\omega_n-E_{+}(k,\phi)][i\hbar\omega_n-E_{-}(k,\phi)]}. \tag{12}$$

For a momentum-independent pairing interaction $V_{kk'}\equiv V$ we obtain the self-consistency equation for $\Delta(\phi)$ from Eq. (5) by summation over ω_n,

$$\frac{1}{N}\sum_k \frac{f(E_{-}(k,\phi))-f(E_{+}(k,\phi))}{2\sqrt{\Delta(\phi)^2+\epsilon^2(k,\phi)}}=\frac{1}{V}, \tag{13}$$

where $f(E)$ denotes the Fermi distribution function. Instead of lowering the temperature we explore below the transition into the superconducting state at zero temperature by increasing the pairing interaction strength V.

The flux ϕ affects the solution of the gap equation [Eq. (13)] for Δ in two ways. For small-size rings the magnitude of Δ is mainly controlled by the energy of the level closest to E_F. If the quantity $\delta_\phi=\min_k|\epsilon(k,\phi)-E_F|>0$, a solution of Eq. (13) exists only above a threshold value of the pairing interaction. In the even-q sectors, this is the case for all values of ϕ, whereas in all odd-q sectors a flux value ϕ exists, for which $\delta_\phi=0$ and Eq. (13) has a solution for all $V>0$ (cf. Fig. 3). This is a consequence of the discreteness of the energy levels. In the strong-coupling regime $V\gg t$, Δ is modulated only slightly by the flux. For weak coupling $V\approx t$, a solution $\Delta_{1/2}<\Delta_c$ is possible in the small-gap regime, where $\Delta_{1/2}$ denotes the order parameter at half-integer flux values. In this case the energy gap closes at a critical flux ϕ_c in the odd-q sectors and $E_{+}(k,\phi)$ turns negative for the level closest to E_F (see Fig. 2). Thus the dominant term in the sum of Eq. (13) switches sign and the solution for Δ vanishes discontinuously. This is equivalent to a breaking of the Cooper pair closest to E_F, which provides the main contribution to the condensation energy.[24,25] These features for the solution of the self-consistency equation are special for strictly 1D rings. In these rings superconductivity is destroyed for velocities of circulating Cooper pairs exceeding the Landau critical velocity, which is approached at $\phi=\phi_c$.[26]

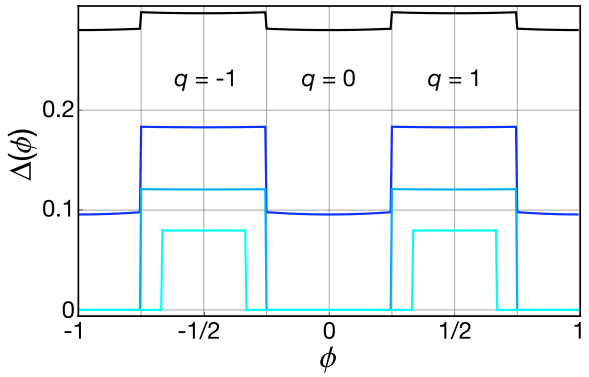

FIG. 3. (Color online) Solution of the self-consistency equation [Eq. (13)] for different values of the pairing energy V at $T=0$. From top to bottom: $V=1.9t, 1.6t, 1.35t, 1.1t$.

With the discrete lattice gradient $\nabla_i f(i)=\frac{1}{2}[f(i+1)-f(i-1)]$, the current is obtained from

$$J(\phi)=\frac{-te}{\hbar}(\nabla_i-\nabla_j)G(i-j)e^{i\varphi_{ij}}\big|_{i=j}=\frac{e}{h}\sum_k\frac{\partial\epsilon_k}{\partial k}n(k), \tag{14}$$

where $n(k)=k_BT\Sigma_n G(k,\omega_n)$ is the momentum distribution function. The result is shown in Fig. 4. For $V=\Delta=0$ one recovers the hc/e-periodic sawtooth pattern for the normal persistent current as discussed in Ref. 22. With increasing Δ, new linear sections appear continuously. These are the sections where the order parameter is finite in the small-gap regime.[19] The occupied state closest to E_F contributes dominantly to the current because all other contributions tend to almost cancel in pairs. The discontinuities of the current occur where the ϕ derivative of the energy of the highest occupied state switches sign (see Fig. 2). These linear sections increase with increasing Δ; once they extend to a range of $hc/2e$ upon reaching the large-gap regime, the current becomes strictly $hc/2e$ periodic.

We obtain further insight into the mechanisms, which determine the current periodicity, by analyzing Δ_c. According to Eq. (11), close to E_F, the maximum energy shift is $t/(2R)$ and the condition for a direct energy gap [or $E_{+}(k,\phi)>0$ for all k and ϕ] and an $hc/2e$-periodic current pattern is there-

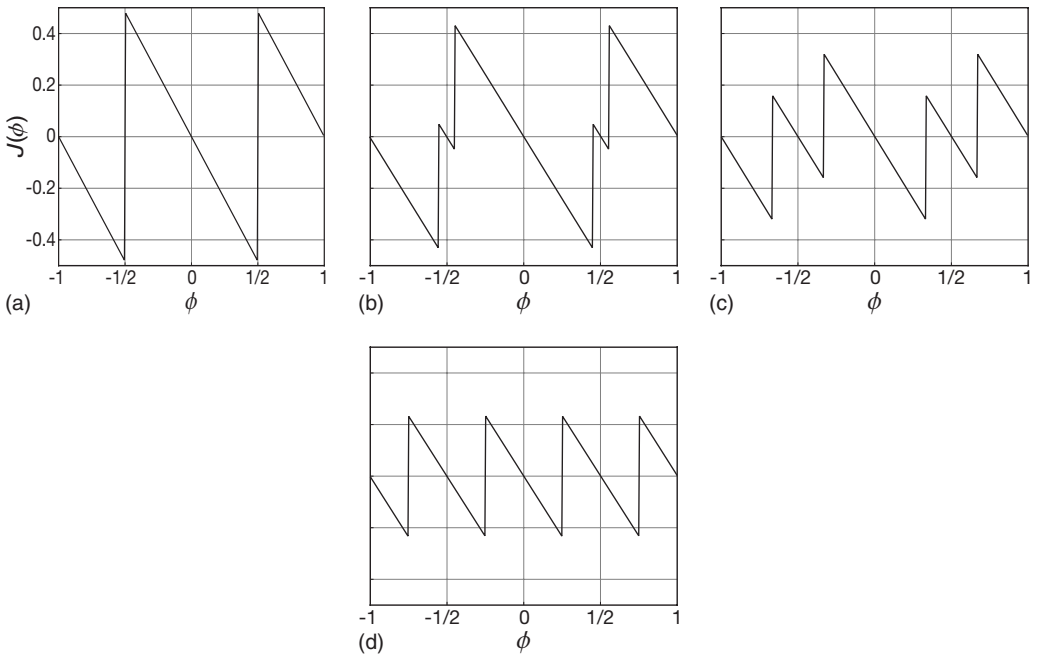

FIG. 4. Crossover from the hc/e-periodic normal persistent current to the $hc/2e$-periodic supercurrent in a ring with $N=26$ at $T=0$. For this ring size $\Delta_c \approx 0.24t$. The discontinuities occur where the ϕ derivative of the highest occupied state energy changes sign.

fore $\Delta > \Delta_c = t/(2R)$. The corresponding critical ring radius is $R_c = t/(2\Delta)$.

It is instructive to compare R_c with the BCS coherence length $\xi_0 = \hbar v_F/(\pi\Delta)$, where v_F is the Fermi velocity and Δ is the BCS order parameter at $T=0$. On the lattice we identify $v_F = \hbar k_F/m$, with $k_F = \pm \pi/2a$ and $m = \hbar^2/(2a^2 t)$; a is the lattice constant. Setting the length unit $a=1$ we obtain $\xi_0 = t/\Delta$ and thus $2R_c = \xi_0$. This signifies that the current response of a superconducting ring smaller than the coherence length is generally hc/e periodic.[15] In these rings the Cooper-pair wave function is delocalized around the ring.

A second fundamental effect, which manifestly breaks the $hc/2e$ periodicity, is the offset of the transition from even to odd center of mass angular momenta q with respect to evenly spaced flux values $(2n-1)hc/4e$. This small offset was already observed in our previous numerical evaluations for d-wave loops.[15] Vakaryuk[21] traced this shift to the dependence of the internal energy of Cooper pairs in the center of mass state. For a BCS-model superconductor, this effect is fully incorporated in the Bogoliubov–de Gennes (BdG) evaluation of Ref. 15 although the quasiparticlelike presentation introduces a different perspective. In the discussion of this section we disregarded the offset for the 1D rings in order to focus on the aspects related to the opening of an indirect gap. In Sec. III we include the offset consistently in the BdG evaluation of the multichannel annulus.

It is worthwhile to note that the condition $\Delta > \Delta_c$ (or $R > R_c$) only refers to the periodicity of the supercurrent. It does not guarantee an $hc/2e$ periodicity of the order parameter Δ or the total energy but only of their derivatives. These quantities need a continuous energy spectrum with degeneracies for flux values which are multiples of $hc/2e$.[6,14]

III. MULTICHANNEL RING: ANNULUS

In this section we describe a superconducting loop of finite width as shown in Fig. 5 with an inner radius R_1 and an outer radius R_2. For such an annulus, we choose a continuum approach on the basis of the BdG equations. For integer and half-integer flux values, these equations can be solved analytically, as we show in Sec. III A. For an arbitrary magnetic flux, we discuss a numerical solution in Sec. III B.

Consider the BdG equations for spin singlet pairing,

$$E_{\mathbf{n}} u_{\mathbf{n}}(\mathbf{r}) = \left[\frac{1}{2m}\left(i\hbar\,\boldsymbol{\nabla} + \frac{e}{c}\mathbf{A}(\mathbf{r})\right)^2 - \mu\right] u_{\mathbf{n}}(\mathbf{r}) + \Delta v_{\mathbf{n}}(\mathbf{r}),$$

$$E_{\mathbf{n}} v_{\mathbf{n}}(\mathbf{r}) = -\left[\frac{1}{2m}\left(i\hbar\,\boldsymbol{\nabla} - \frac{e}{c}\mathbf{A}(\mathbf{r})\right)^2 - \mu\right] v_{\mathbf{n}}(\mathbf{r}) + \Delta^* u_{\mathbf{n}}(\mathbf{r}), \tag{15}$$

with the self-consistency condition (gap equation) for the order parameter $\Delta(\mathbf{r})$,

$$\Delta(\mathbf{r}) = V \sum_{\mathbf{n}} u_{\mathbf{n}}(\mathbf{r}) v_{\mathbf{n}}^*(\mathbf{r}) \tanh\left(\frac{E_{\mathbf{n}}}{2T}\right), \tag{16}$$

where V is the local pairing potential. For an annulus of finite width we separate the angular part of the quasiparticle wave functions $u_{\mathbf{n}}(\mathbf{r})$ and $v_{\mathbf{n}}(\mathbf{r})$ using polar coordinates $\mathbf{r} = (r, \varphi)$ and the ansatz,

$$u_{\mathbf{n}}(r,\varphi) = u_{\mathbf{n}}(r) e^{i(k+q)\varphi/2},$$

$$v_{\mathbf{n}}(r,\varphi) = v_{\mathbf{n}}(r) e^{i(k-q)\varphi/2} \tag{17}$$

where k and q are either both even or both odd integers. Thus $\hbar k$ is the angular momentum as for the 1D ring and $\mathbf{n}$

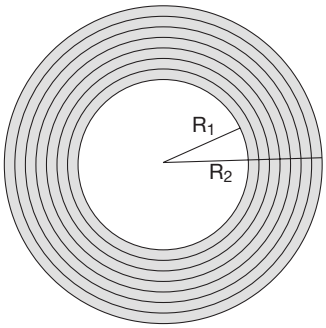

FIG. 5. Annulus with inner radius R_1 and outer radius R_2. For a magnetic flux threading the interior of the annulus, the radial part of the Bogoliubov–de Gennes equations is solved numerically with a discretized radial coordinate.

$=(k,\rho)$ with the radial quantum number ρ. The order parameter factorizes into $\Delta(r,\varphi)=\Delta(r)e^{iq\varphi}$, where the radial component

$$\Delta(r) = V\sum_{\mathbf{n}} u_{\mathbf{n}}(r)v_{\mathbf{n}}^{*}(r)\tanh\left(\frac{E_{\mathbf{n}}}{2T}\right) \tag{18}$$

is real. For a magnetic flux Φ threading the interior of the annulus we choose the vector potential $\mathbf{A}(r,\varphi)=\mathbf{e}_{\varphi}\Phi/(2\pi r)$, where $\mathbf{e}_{\varphi}$ is the azimuthal unit vector. With $\phi=(e/hc)\Phi$ and

$$\left(-i\boldsymbol{\nabla} \pm \frac{\phi}{r}\mathbf{e}_{\varphi}\right)^2 = -\frac{1}{r}\partial_r(r\partial_r) + \frac{1}{r^2}(-i\partial_{\varphi} \pm \phi)^2, \tag{19}$$

the BdG equations therefore reduce to radial differential equations for $u_{\mathbf{n}}(r)$ and $v_{\mathbf{n}}(r)$,

$$E_{\mathbf{n}}u_{\mathbf{n}}(r) = -\left[\frac{\hbar^2}{2m}\frac{\partial_r}{r}(r\partial_r) - \frac{\hbar^2 l_u^2}{2mr^2} + \mu\right]u_{\mathbf{n}}(r) + \Delta(r)v_{\mathbf{n}}(r),$$

$$E_{\mathbf{n}}v_{\mathbf{n}}(r) = \left[\frac{\hbar^2}{2m}\frac{\partial_r}{r}(r\partial_r) - \frac{\hbar^2 l_v^2}{2mr^2} + \mu\right]v_{\mathbf{n}}(r) + \Delta(r)u_{\mathbf{n}}(r), \tag{20}$$

with the canonical angular momenta,

$$\hbar l_u = \frac{\hbar}{2}(k+q-2\phi), \tag{21}$$

$$\hbar l_v = \frac{\hbar}{2}(k-q+2\phi). \tag{22}$$

The number q plays the same role as in Sec. II. Here we choose q for each value of the flux to minimize the total energy of the system. The flux for which q changes to the next integer can therefore deviate from the values $(2n-1)/4$, where we fixed the change in q for the 1D model.

A. Hankel-function ansatz

A natural choice of an ansatz for the solutions of the coupled differential equations [Eq. (20)] are linear combinations of the Hankel functions, $H_l^{(1)}$ and $H_l^{(2)}$, since they are individually solutions of the uncoupled Eq. (20) for $\Delta(r)=0$;

$$\left(\frac{1}{r}\partial_r(r\partial_r) - \frac{l^2}{r^2}\right)H_l^{(1,2)}(\gamma r) = \gamma^2 H_l^{(1,2)}(\gamma r). \tag{23}$$

We therefore take $u_{\mathbf{n}}(r)$ and $v_{\mathbf{n}}(r)$ of the form

$$u_{\mathbf{n}}(r) = u_{\mathbf{n}}[H_{l_u}^{(1)}(\gamma_{\mathbf{n}}^{\mu}r) + c_{\mathbf{n}}^{u}H_{l_u}^{(2)}(\gamma_{\mathbf{n}}^{\mu}r)], \tag{24}$$

$$v_{\mathbf{n}}(r) = v_{\mathbf{n}}[H_{l_v}^{(1)}(\gamma_{\mathbf{n}}^{v}r) + c_{\mathbf{n}}^{v}H_{l_v}^{(2)}(\gamma_{\mathbf{n}}^{v}r)]. \tag{25}$$

Equation (20) then becomes

$$E_{\mathbf{n}}u_{\mathbf{n}}(r)] = -\left[\frac{\hbar^2}{2m}(\gamma_{\mathbf{n}}^{\mu})^2 + \mu\right]u_{\mathbf{n}}(r) + \Delta(r)v_{\mathbf{n}}(r),$$

$$E_{\mathbf{n}}v_{\mathbf{n}}(r) = \left[\frac{\hbar^2}{2m}(\gamma_{\mathbf{n}}^{v})^2 + \mu\right]v_{\mathbf{n}}(r) + \Delta(r)u_{\mathbf{n}}(r). \tag{26}$$

The coefficients $\gamma_{\mathbf{n}}^{\alpha}$ and $c_{\mathbf{n}}^{\alpha}$, with $\alpha=u,v$, are fixed by the open boundary conditions, for which $u_{\mathbf{n}}(r)$ and $v_{\mathbf{n}}(r)$ vanish on the inner and outer boundaries of the annulus: $u_{\mathbf{n}}(R_1)=u_{\mathbf{n}}(R_2)=0$ and $v_{\mathbf{n}}(R_1)=v_{\mathbf{n}}(R_2)=0$. This generates the defining equations for $\gamma_{\mathbf{n}}^{\alpha}$ and $c_{\mathbf{n}}^{\alpha}$,

$$c_{\mathbf{n}}^{\alpha} = -\frac{H_{l_\alpha}^{(1)}(\gamma_{\mathbf{n}}^{\alpha}R_1)}{H_{l_\alpha}^{(2)}(\gamma_{\mathbf{n}}^{\alpha}R_1)} = -\frac{H_{l_\alpha}^{(1)}(\gamma_{\mathbf{n}}^{\alpha}R_2)}{H_{l_\alpha}^{(2)}(\gamma_{\mathbf{n}}^{\alpha}R_2)}. \tag{27}$$

For all integer and half-integer values of flux, $q=2\phi$ in the ground state; thus $l_u=l_v=k/2$. Assuming a constant order parameter $\Delta(r)=\Delta$, the r dependence drops out from Eq. (26), and we find the eigenvalues and eigenvectors of the usual BCS type,

$$E_{\mathbf{n}} = \sqrt{\left(\frac{\hbar^2}{2m}\gamma_{\mathbf{n}}^2 - \mu\right)^2 + \Delta^2}, \tag{28}$$

with $\gamma_{\mathbf{n}}=\gamma_{\mathbf{n}}^{\mu}=\gamma_{\mathbf{n}}^{v}$ and

$$u_{\mathbf{n}} = \frac{1}{2}\left[1 + \left(\frac{\hbar^2}{2m}\gamma_{\mathbf{n}}^2 + \mu\right)/E_{\mathbf{n}}\right], \tag{29}$$

$$v_{\mathbf{n}} = \frac{1}{2}\left[1 - \left(\frac{\hbar^2}{2m}\gamma_{\mathbf{n}}^2 + \mu\right)/E_{\mathbf{n}}\right]. \tag{30}$$

These are the two distinct classes of superconducting states as discussed for the 1D loop: for integer flux values, Δ is given by summing over all even angular momenta k, whereas for half-integer flux values, Δ is obtained by summing over odd angular momenta.

For general values of magnetic flux, l_u and l_v are different and so are $\gamma_{\mathbf{n}}^{\mu}$ and $\gamma_{\mathbf{n}}^{v}$. The r dependence of $u_{\mathbf{n}}(r)$ is therefore different from $v_{\mathbf{n}}(r)$ as contained in Eqs. (24) and (25). In the Appendix we analyze the solution of the uncoupled Eq. (20) for $\Delta=0$ and find that the eigenfunctions account for the flux-induced Doppler shift by shifting their nodes closer together or further apart—most importantly, $u_{\mathbf{n}}(r)$ shifts its nodes in the opposite direction than those in $v_{\mathbf{n}}(r)$. This im-

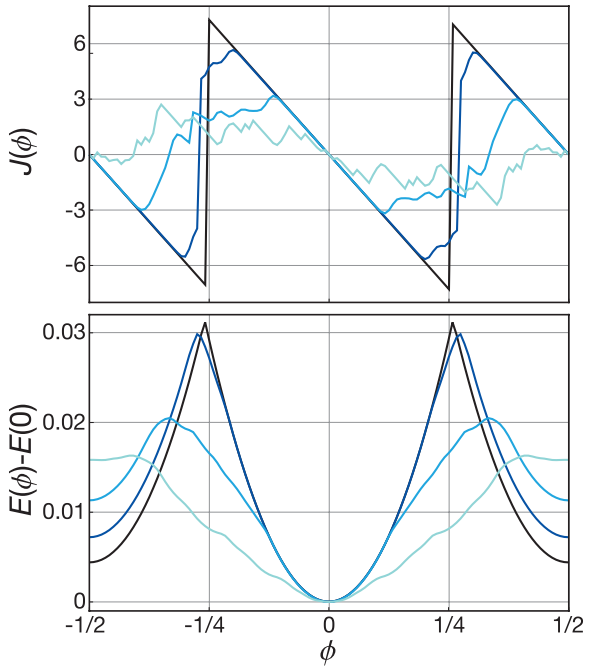

FIG. 6. (Color) Non-self-consistent calculation of current and energy at $T=0$. The circulating current (upper panel) in an annulus with an inner radius $R_1=100a$ and an outer radius $R_2=150a$ is shown for fixed, ϕ independent $\Delta=0$ (light blue line), $\Delta=0.002t$ (blue line), $\Delta=0.004t$ (dark blue line), and $\Delta=0.006t$ (black line). The lower panel shows the difference between the total energy of the annulus as a function of ϕ and the total energy at zero flux for the same values for Δ as above.

plies that $u_{\mathbf{n}}(r)$ and $v_{\mathbf{n}}(r)$ with the ansatz of Eqs. (24) and (25) cannot be solutions of the coupled Eq. (26) for $\Delta(r) \neq 0$.

Moreover, we show in the Appendix for the limit of a thin annulus ($R_1 \gg R_2 - R_1$) that both the Doppler shift and the shift of the nodes of $u_{\mathbf{n}}(r)$ and $v_{\mathbf{n}}(r)$ are in leading-order linear functions of $q-2\phi$. It is therefore not possible to find an approximate solution of Eq. (20) that contains the effects of the Doppler shift but neglects the shift of the nodes. Consequently, we have to resort to a numerical solution of the radial component of the BdG equations.

B. Self-consistent numerical solution

The numerical solution of Eq. (20) is achieved by discretizing the interval $[R_1, R_2]$ for the radial coordinate r into M radii r_i, which defines the grid constant $a=(R_2-R_1)/M$. In this way we obtain for each angular momentum $\hbar k$ M radial eigenstates (channels), which correspond to the M eigenstates with the lowest eigenenergies $E_{\mathbf{n}}$ of the continuum model. On this set of M radial coordinates, we use the symmetric discrete differential operators $\partial_i f(r_i)=[f(r_{i+1}) - f(r_{i-1})]/a$ and $\partial_i^2 f(r_i)=[f(r_{i+1})+f(r_{i-1})-2f(r_i)]/a^2$. Inserting these discrete operators into Eq. (20) and using $(1/r)\partial_r r \partial_r = (1/r)\partial_r + \partial_r^2$, one obtains the eigenvalue equation,

$$\begin{pmatrix} \hat{t} + \hat{\mu}_k^u & \hat{\Delta} \\ \hat{\Delta} & -\hat{t} - \hat{\mu}_k^v \end{pmatrix} \begin{pmatrix} u_{\mathbf{n}} \\ v_{\mathbf{n}} \end{pmatrix} = E_{\mathbf{n}} \begin{pmatrix} u_{\mathbf{n}} \\ v_{\mathbf{n}} \end{pmatrix}, \tag{31}$$

where $u_{\mathbf{n}}$ and $v_{\mathbf{n}}$ are real and the operators $\hat{t}$, $\hat{\mu}_k^\alpha$, and $\hat{\Delta}$ are defined through

$$\hat{t}u_{\mathbf{n}}(r_i) = t[u_{\mathbf{n}}(r_{i+1}) + u_{\mathbf{n}}(r_{i-1})] + t\frac{a}{r_i}[u_{\mathbf{n}}(r_{i+1}) - u_{\mathbf{n}}(r_{i-1})], \tag{32}$$

and

$$\hat{\mu}_k^\alpha u_{\mathbf{n}}(r_i) = t\left[\frac{a^2}{r_i^2} l_\alpha^2 - 2\right] u_{\mathbf{n}}(r_i), \tag{33}$$

$$\hat{\Delta} u_{\mathbf{n}}(r_i) = \Delta(r_i) u_{\mathbf{n}}(r_i), \tag{34}$$

where $t=\hbar^2/(2ma^2)$. A self-consistent solution of Eq. (31) and the gap equation,

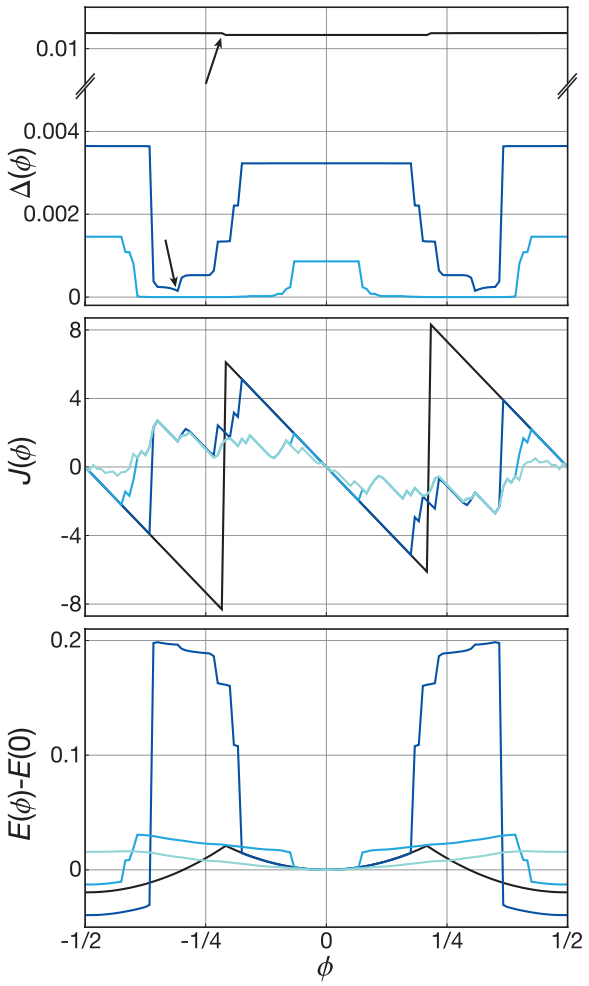

FIG. 7. (Color) Self-consistent calculations for the same annulus as in Fig. 6. In addition, the top panel displays the self-consistent order parameter Δ as a function of ϕ. The lines correspond to the pairing interaction $V=0$ (light blue line), $V=0.28t$ (blue line), $V=0.32t$ (dark blue line), and $V=0.38t$ (black line). The black arrows mark the positions of the q jump for $V=0.38t$ and $V=0.32t$.

$$\Delta(r_i) = V\sum_{\mathbf{n}} u_{\mathbf{n}}(r_i)v_{\mathbf{n}}(r_i)\tanh\left(\frac{E_{\mathbf{n}}}{2T}\right), \tag{35}$$

is found iteratively. The operator $\hat{t}$ consists of a symmetric and an antisymmetric part with respect to r_{i-1} and r_{i+1}. In order to ensure that the eigenvalues of Eq. (31) are real, the prefactor of the second antisymmetric term in Eq. (32) must be smaller or equal to the prefactor of the symmetric term, which means $M \geq (R_2-R_1)/2R_1$. This condition is fulfilled since $M=(R_2-R_1)/a > (R_2-R_1)/2R_1$.

Once the eigenfunctions of Eq. (31) are known, we obtain the current by evaluating the expectation value of the gauge-invariant current operator.[24] The expectation value $J(r)$ of the circulating current is found using a Bogoliubov transformation and ansatz (17) in polar coordinates;

$$J(r) = \frac{\hbar e}{m}\sum_{\mathbf{n}}[J^u_{\mathbf{n}}(r)f(E_{\mathbf{n}}) - J^v_{\mathbf{n}}(r)f(-E_{\mathbf{n}})], \tag{36}$$

with

$$J^{\alpha}_{\mathbf{n}}(r) = \frac{\hbar e}{m}\mathrm{Im}\left[\alpha^*_{\mathbf{n}}(r,\varphi)\left(-\frac{i}{r}\partial_{\varphi} - \frac{\phi}{r}\right)\alpha_{\mathbf{n}}(r,\varphi)\right] = \frac{\hbar e}{m}\frac{l_{\alpha}}{r}\alpha^2_{\mathbf{n}}(r) \tag{37}$$

for $\alpha=u,v$. The contribution of each quasiparticle state to the total current is therefore determined by its angular velocity l_{α}. The radial quantum number ρ and the Δ dependence enter only through the occupation probability which is controlled by the eigenenergy $E_{\mathbf{n}}$. Further, the total energy of the system is given by

$$E = \frac{1}{M}\sum_{\mathbf{n}} E_{\mathbf{n}}\sum_i [u^2_{\mathbf{n}}(r_i)f(E_{\mathbf{n}}) + v^2_{\mathbf{n}}(r_i)f(-E_{\mathbf{n}})]. \tag{38}$$

C. Results

The results of the non-self-consistent calculations for the circulating current and the total energy at $T=0$ and for fixed values of Δ are displayed in Fig. 6. In the normal state ($\Delta=0$), there are $\sim M$ eigenstates close enough to E_F to cross E_F as a function of ϕ, unlike in small 1D rings where only one state crosses E_F. For each crossing, a small jump appears in the current as a function of ϕ. There is a larger jump at the value of ϕ where the energies of the even-q and odd-q states become degenerate and q switches to the next integer. The shape of this function depends on the distribution of eigenenergies close to E_F and therefore on microscopic details of the geometry of the annulus and the Fermi energy E_F. A finite Δ allows for a flux regime with direct energy gap and no crossings of E_F; thus in this regime the current is linear and the total-energy quadratic in ϕ. For the largest value ($\Delta=0.006t$) shown, there is a direct gap for all values of ϕ. Even for this value of Δ, the current and the energy are not exactly $hc/2e$ periodic because of the energy difference of the even-q and odd-q states in finite systems.[12,15]

The introduction of self-consistency in Δ does not fundamentally change these basic observations (Fig. 7). The crossover is then controlled by the pairing interaction strength V, for which we chose such values as to reproduce the crossover from the normal state to a state with direct energy gap for all flux values. The order parameter Δ is now a function of ϕ. If $\Delta(\phi=0) \lesssim 0.006t$ (cf. Fig. 6), the gap closes with ϕ and Δ decreases whenever a state crosses E_F. At these flux values we observe a sharp increase in the total energy of the annulus. Unlike in 1D, Δ does not drop to zero at the closing of the energy gap but decreases stepwise. In two or three dimensions, Δ remains finite beyond ϕ_c because it is stabilized by contributions to the condensation energy from pairs with relative momenta perpendicular to the direction of the current flow and the closing of the indirect energy gap does not destroy superconductivity.[25,26] Apart from these steps, the current (energy) shows the standard linear (quadratic) behavior.

The offset of the q jump is only relevant for values of V for which Δ is finite for all ϕ. In Fig. 7, the offset is clearly visible for the largest two values of V (marked with black arrows). Its sign depends on the geometry of the annulus and the pairing interaction V—the offset changes sign for increasing V (cf. Ref. 21).

Experimentally more relevant is to control the crossover through temperature. With the pairing interaction V sufficiently strong to produce a $T=0$ energy gap much larger than the maximum Doppler shift, the crossover regime is reached for temperatures slightly below T_c. For the annulus described in Fig. 8, the crossover proceeds within approximately 1% of T_c. The crossover regime gets narrower for larger rings proportional to the decrease in the Doppler shift. In the limit of a quasi-1D ring of radius R we can be more precise. If we define the crossover temperature T^* by $\Delta(T^*)=\Delta_c$ and assuming $\Delta_c \ll \Delta$, we can use the Ginzburg-Landau form of the order parameter,

$$\frac{\Delta(T)}{\Delta(0)} \approx 1.75\sqrt{1-\frac{T}{T_c}}, \tag{39}$$

and obtain

$$\frac{T_c - T^*}{T_c} \approx \frac{\Delta_c^2}{3.1\Delta(0)^2} = \frac{t^2}{12.4\Delta(0)^2R^2} = \frac{E_F^2}{3.1T_c^2R^2}. \tag{40}$$

For a ring with a radius of 2500 lattice constants (≈ 10 μm) and $\Delta(0)=0.01t$ (≈ 3 meV), one finds the ratio $(T_c-T^*)/T_c \approx 1.3\times 10^{-4}$. This is in reasonable qualitative agreement with the experimental results of Little and Parks,[9,10] discussed also by Tinkham.[27] Their theoretical prediction is similar to Eq. (40), up to a factor in which they include a finite mean-free path. Moreover, they do not include the difference introduced through even-q and odd-q states. This difference was considered in the calculations of T_c by Bogachek *et al.*[13] in the one-channel limit. In Eq. (40) the value of $\Delta(0)$ is in fact different for even and odd q's. Although quantitative predictions of T_c-T^* of the theory presented here might be too large compared to the experiment, it serves as an upper limit because it describes the maximum possible persistent current. Scattering processes in real systems will further reduce T_c-T^*.

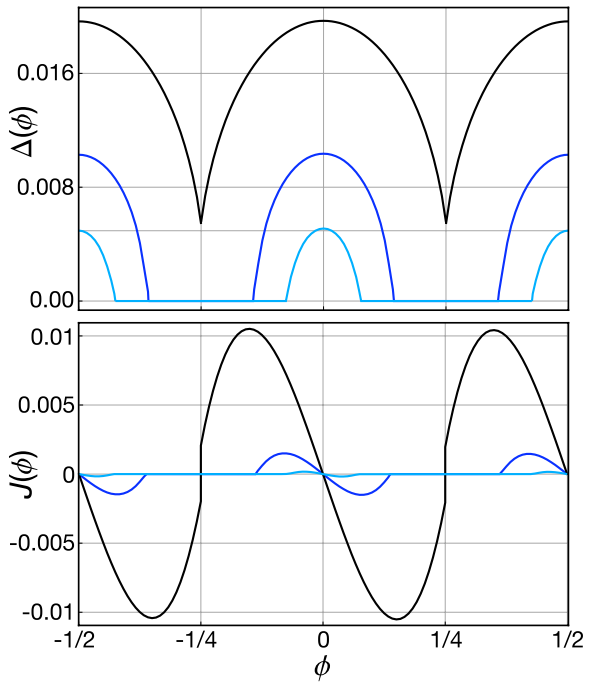

FIG. 8. (Color online) The order parameter Δ and the persistent current for the temperature-driven transition from the normal to the superconducting state in an annulus with inner radius $R_1=30a$ and outer radius $R_2=36a$. The pairing intercation is $V=0.7t$, with a critical temperature of $T_c\approx 0.0523t$ for zero flux. For these parameters $\Delta(T=0)\approx 0.1t$. The lines (from top to bottom) correspond to the temperatures $T=0.0513t$, $T=0.0520t$, and $T=0.0522t$. Notice that Δ is slightly different for the flux values $\phi=0$ and $\pm 1/2$.

For temperatures close to T_c, the difference of the eigenenergies of even-q and odd-q states is less important than at $T=0$. Thus the deviation from the hc/e periodicity of the current and of the order parameter is smaller. Furthermore, persistent currents in the normal state are exponentially small compared to the persistent supercurrents below T_c. Their respective hc/e-periodic behavior is therefore essentially invisible in the flux regime where $\Delta=0$. For the annulus described in Fig. 8, the difference between $\Delta(\phi=0)$ and $\Delta(\phi=1/2)$ is still visible, but the corresponding differences in the current are too small.

IV. CONCLUSIONS

We have described the crossover from the hc/e-periodic persistent currents as a function of magnetic flux in a metallic loop to the $hc/2e$-periodic persistent supercurrent in a 1D loop as well as in a multichannel annulus. While a 1D superconducting ring is a rather idealized system, it proves valuable for discussing the physics of this crossover. A ring with a radius smaller than half the superconducting coherence length shows an hc/e-periodic supercurrent, which reaches the critical current at a critical flux value ϕ_c, determined by the flux-dependent closing of the gap. Assuming that this relation remains unchanged on a ring with finite thickness $d \ll R$, as indeed suggested by the multichannel model, R_c would be of the order of 1 μm for aluminum rings. In two or three dimensions, Δ remains finite beyond ϕ_c. The temperature-controlled crossover, while cooling through T_c, appears within a temperature window proportional to $1/R^2$ and thus appears hard to detect in experiment.

ACKNOWLEDGMENTS

We are grateful to Yuri Barash, John Kirtley, Jochen Mannhart, Douglas Scalapino, and Christof Schneider for useful discussions. T.K. is grateful for the kind hospitality at the Aspen Center for Physics where this work was discussed. This work was supported by the Deutsche Forschungsgemeinschaft through Grant No. SFB 484 and by the EC (Nanoxide).

APPENDIX: DOPPLER SHIFT AND NODES OF THE HANKEL-FUNCTION ANSATZ

The ansatz for $u_{\mathbf{n}}(r)$ and $v_{\mathbf{n}}(r)$ with two Hankel functions [Eqs. (24) and (25)] solves the normal-state Schrödinger equation for the annulus as well as the BdG equations in the superconducting state with integer and half-integer flux values. In this appendix we show that it is not possible to construct an approximate analytic solution for the superconducting annulus that includes the effect of the Doppler shift. In this case $u_{\mathbf{n}}(r)$ and $v_{\mathbf{n}}(r)$ have the independent eigenenergies $(\hbar^2/2m)(\gamma_{\mathbf{n}}^u)^2$ and $(\hbar^2/2m)(\gamma_{\mathbf{n}}^v)^2$.

For this purpose we analyze the relation between the Doppler shift of the eigenfunctions of the annulus in the normal state ($\Delta=0$) and the shift of their nodes with respect to the radial coordinate using the following asymptotic form for the Hankel functions:[28]

$$H_l^{(1,2)}\left(\frac{l}{\cos x}\right)=\sqrt{\frac{2}{\pi l\tan x}}\exp\left[\pm i\left(l\tan x-lx-\frac{\pi}{4}\right)\right], \tag{A1}$$

which approximates $H_l^{(1)/(2)}$ for $l\gg 1$. Choosing $x=\arccos(l/\gamma r)$ leads with $\tan(\arccos x)=\sqrt{1-x^2}/x$ to

$$H_l^{(1,2)}(\gamma r)=\sqrt{\frac{2}{\pi l}}\left[\left(\frac{\gamma r}{l}\right)^2-1\right]^{-1/4}\times\exp\left[\pm i\left(r\sqrt{\gamma^2-\frac{l^2}{r^2}}-l\arccos\frac{l}{\gamma r}-\frac{\pi}{4}\right)\right]. \tag{A2}$$

Thus Eq. (A2) approximates $H_l^{(1,2)}(\gamma r)$ for $\gamma r\gg 1$. Inserting Eq. (A2) into the boundary conditions [Eq. (27)] determines the constants $c_{\mathbf{n}}^{\alpha}$ and $\gamma_{\mathbf{n}}^{\alpha}$;

$$c_{\mathbf{n}}^{\alpha}=\exp\left[2i\left(D_{\mathbf{n}}^{\alpha}(R_1)-\frac{\pi}{4}\right)\right]=\exp\left[2i\left(D_{\mathbf{n}}^{\alpha}(R_2)-\frac{\pi}{4}\right)\right], \tag{A3}$$

with

$$D_{\mathbf{n}}^{\alpha}(r) = r\sqrt{(\gamma_{\mathbf{n}}^{\alpha})^2 - \frac{l_{\alpha}^2}{r^2}} - l_{\alpha}\arccos\frac{l_{\alpha}}{\gamma_{\mathbf{n}}^{\alpha} r}. \tag{A4}$$

The wave functions $u_{\mathbf{n}}(r)$ and $v_{\mathbf{n}}(r)$ [Eqs. (24) and (25)] become

$$u_{\mathbf{n}}(r) = u_{\mathbf{n}}\sqrt{\frac{8}{\pi l_u}}\left[\left(\frac{\gamma_{\mathbf{n}}^{\mu} r}{l_u}\right)^2 - 1\right]^{-1/4} \times e^{i[D_{\mathbf{n}}^{u}(R_1)+\pi/4]}\sin[D_{\mathbf{n}}^{u}(r) - D_{\mathbf{n}}^{u}(R_1)], \tag{A5}$$

$$v_{\mathbf{n}}(r) = v_{\mathbf{n}}\sqrt{\frac{8}{\pi l_v}}\left[\left(\frac{\gamma_{\mathbf{n}}^{v} r}{l_v}\right)^2 - 1\right]^{-1/4} \times e^{i[D_{\mathbf{n}}^{v}(R_1)+\pi/4]}\sin[D_{\mathbf{n}}^{v}(r) - D_{\mathbf{n}}^{v}(R_1)]. \tag{A6}$$

The vanishing of the wave function for $r=R_2$ therefore implies that

$$D_{\mathbf{n}}^{\alpha}(R_2) - D_{\mathbf{n}}^{\alpha}(R_1) = -\pi\rho \tag{A7}$$

for an integer ρ, which determines $\gamma_{\mathbf{n}}^{\alpha}$. In the limit of a thin annulus ($R_1 \gg R_2 - R_1$), we expand $D_{\mathbf{n}}^{\alpha}(r)$ in $1/r$ and find

$$D_{\mathbf{n}}^{\alpha}(r) - D_{\mathbf{n}}^{\alpha}(R_1) \approx (r - R_1)\left[\gamma_{\mathbf{n}}^{\alpha} - \frac{l_{\alpha}^2}{2\gamma_{\mathbf{n}}^{\alpha} r R_1}\right]. \tag{A8}$$

With this asymptotic form the boundary condition (A7) becomes a quadratic equation in $\gamma_{\mathbf{n}}^{\alpha}$,

$$(\gamma_{\mathbf{n}}^{\alpha})^2 - \frac{\pi\rho}{R_1 - R_2}\gamma_{\mathbf{n}}^{\alpha} - \frac{l_{\alpha}^2}{2R_1 R_2} = 0, \tag{A9}$$

which has the positive solution,

$$\gamma_{\mathbf{n}}^{\alpha} = \frac{1}{2}\left[\frac{\pi\rho}{R_1 - R_2} + \sqrt{\left(\frac{\pi\rho}{R_1 - R_2}\right)^2 + \frac{l_{\alpha}^2}{2R_1 R_2}}\right]. \tag{A10}$$

This is the simplest possible approximation for the eigenenergies of the uncoupled equations ($\Delta=0$) of the annulus containing the Doppler shift, which is controlled by l_{α}^2. The flux ϕ enters l_u and l_v with different signs [see Eq. (22)]. Thus, if $\gamma_{\mathbf{n}}^{\mu}$ decreases as a function of ϕ, $\gamma_{\mathbf{n}}^{v}$ increases. Since $q-2\phi < 1$ in the ground state, the Doppler shift $(\hbar^2/2m)[(\gamma_{\mathbf{n}}^{\alpha})^2(q-2\phi) - (\gamma_{\mathbf{n}}^{\alpha})^2(0)]$ is linear in leading order in $(q-2\phi)/\sqrt{R_1}$.

We further find the nodes $r_{\mathbf{n}m}$ of $u_{\mathbf{n}}(r)$ and $v_{\mathbf{n}}(r)$ by setting expression (A8) equal to πm, where m is a positive integer, and solving it for $r>0$,

$$r_{\mathbf{n}m} = \frac{1}{2}\left[R_1 + \frac{l_{\alpha}^2}{2(\gamma_{\mathbf{n}}^{\alpha})^2 R_1} - \frac{\pi m}{\gamma_{\mathbf{n}}^{\alpha}} + \sqrt{\left(R_1 + \frac{l_{\alpha}^2}{2(\gamma_{\mathbf{n}}^{\alpha})^2 R_1} - \frac{\pi m}{\gamma_{\mathbf{n}}^{\alpha}}\right)^2 - \frac{2l_{\alpha}^2}{(\gamma_{\mathbf{n}}^{\alpha})^2}}\right]. \tag{A11}$$

The shift of the nodes $r_{\mathbf{n}m}(q-2\phi) - r_{\mathbf{n}m}(0)$ as a function of flux is again linear in $(q-2\phi)/\sqrt{R_1}$ to leading order. Thus both the Doppler shift and the nodes of $u_{\mathbf{n}}(r)$ shift linearly with ϕ and conversely when compared with the Doppler shift and the nodes of $v_{\mathbf{n}}(r)$.

The coupled Eq. (26) for $\Delta \neq 0$ resulting from ansatz (24) and (25) with noninteger (or non-half-integer) flux can be solved only by wave functions $u_{\mathbf{n}}(r)$ and $v_{\mathbf{n}}(r)$ with the same r dependence. To obtain a solution of this problem, one can expand the wave functions as a sum of Hankel functions and numerically solve for the coefficients or directly solve the coupled differential equations numerically.

[1] Y. Aharonov and D. Bohm, Phys. Rev. **115**, 485 (1959).
[2] M. Büttiker, Y. Imry, and R. Landauer, Phys. Lett. **96A**, 365 (1983).
[3] R. Landauer and M. Büttiker, Phys. Rev. Lett. **54**, 2049 (1985).
[4] F. London, *Superfluids* (Wiley, New York, 1950).
[5] N. Byers and C. N. Yang, Phys. Rev. Lett. **7**, 46 (1961).
[6] J. R. Schrieffer, *Theory of Superconductivity* (Addison-Wesley, Reading, MA, 1964), Chap. 8.
[7] R. Doll and M. Näbauer, Phys. Rev. Lett. **7**, 51 (1961).
[8] B. S. Deaver and W. M. Fairbank, Phys. Rev. Lett. **7**, 43 (1961).
[9] W. A. Little and R. D. Parks, Phys. Rev. Lett. **9**, 9 (1962).
[10] R. D. Parks and W. A. Little, Phys. Rev. **133**, A97 (1964).
[11] U. Essmann and H. Träuble, Phys. Lett. **24A**, 526 (1967).
[12] P. G. de Gennes, *Superconductivity of Metals and Alloys* (Addison-Wesley, Reading, MA, 1966), Chap. 5.
[13] E. N. Bogachek, G. A. Gogadze, and I. O. Kulik, Phys. Status Solidi B **67**, 287 (1975).
[14] W. Brenig, Phys. Rev. Lett. **7**, 337 (1961).
[15] F. Loder, A. P. Kampf, T. Kopp, J. Mannhart, C. W. Schneider, and Y. S. Barash, Nat. Phys. **4**, 112 (2008).
[16] Y. S. Barash, Phys. Rev. Lett. **100**, 177003 (2008).
[17] V. Juričić, I. F. Herbut, and Z. Tešanović, Phys. Rev. Lett. **100**, 187006 (2008).
[18] J.-X. Zhu, arXiv:0806.1084 (unpublished).
[19] K. Czajka, M. M. Maśka, M. Mierzejewski, and Z. Śledź, Phys. Rev. B **72**, 035320 (2005).
[20] T.-C. Wei and P. M. Goldbart, Phys. Rev. B **77**, 224512 (2008).
[21] V. Vakaryuk, Phys. Rev. Lett. **101**, 167002 (2008).
[22] H. F. Cheung, Y. Gefen, E. K. Riedel, and W. H. Shih, Phys. Rev. B **37**, 6050 (1988).
[23] V. P. Mineev and K. V. Samokhin, *Introduction to Unconventional Superconductivity* (Gordon and Breach, New York, 1999), Chap. 17.
[24] P. F. Bagwell, Phys. Rev. B **49**, 6841 (1994).
[25] J. Bardeen, Rev. Mod. Phys. **34**, 667 (1962).
[26] A. M. Zagoskin, *Quantum Theory of Many-Body Systems* (Springer, New York, 1998), Chap. 4.
[27] M. Tinkham, Phys. Rev. **129**, 2413 (1963).
[28] M. Abramowitz and A. Stegun, *Pocketbook of Mathematical Functions* (Harri Deutsch Verlag, Thun, 1984).